

DEVELOPMENT OF AN EXPERIMENTAL FACILITY FOR CROSS FLOW WATER TURBINE MODELS

Vivien AUMELAS¹, Thierry MAITRE²

Within the framework of the HARVEST project, a new concept of cross flow water turbine (CFWT) is developed. To optimize experimentally the turbine shape and also to validate the numerical modelling of the flow, the LEGI hydrodynamic tunnel has been equipped with a multi component measurement platform. This device allows measuring the static and dynamic components of the longitudinal and transversal thrusts applied on turbine models (scale 1/5) as well as the delivered instantaneous torque. This paper presents firstly the global architecture of the measuring chain. Secondly, the validation of the measurement platform is discussed. A rigorous method based on permanent magnets is detailed in order to determine thrust uncertainties. Finally, the use of this experimental facility is illustrated by testing three different cross flow turbines.

Keywords: Experimental hydrodynamic tunnel, cross flow water turbine.

1. Introduction

In response to the exhaustion of fossil energies, the constant growth of energetic needs and environmental interests, several new renewable energies were born during the last century. Systems using water current energies are among the most promising ones. Cross Flow Water Turbines (CFWT) are a solution type. The first CFWT was proposed in 1931 by G. Darrieus [1].

Since twenty years, the Darrieus water turbines have been the object of many experimental surveys in laboratory. In order to characterize the behaviour of CFWTs in rotation, some experimental apparatus have been developed. The experimental bench of Kyushu University [2 - 4], provides the average and instantaneous torque measurements of CFWT for a gravitational flow in a rectangular duct. In addition, for each blade of the turbine, the tangential and normal efforts are supplied by the measuring chain every 10 rotational degrees. The experimental apparatus of the Nihon University [5] allows characterizing only the average and instantaneous torque of a CFWT in a free stream flow. B. Kirke in [6], provides the measurement of the average torque for two CWFTs, one with straight blades, the other one with helical blades. T. Faure in [7] studies, in particular, the influence of the foil section and the number of blades on the

¹ PhD. Student, Laboratory of Geophysical and Industrial Fluid Flows (LEGI), Grenoble, France

² Assoc. Prof. Institut National Polytechnique de Grenoble (INPG), LEGI, Grenoble, France.

efficiency of CWFTs. However, for each aforementioned study, uncertainties on the measuring chain are not discussed.

The Sandia National Laboratory and the National Research Council of Canada provide the average and instantaneous torque measurements for a Darrieus turbine in air flow. The results are listed by I. Paraschivoiu in [8]. It is noticed that torque and effort measurements in air are easier than in water. Nevertheless, as Y. Takamatsu in [2], water studies of CWFTs allow characterizing the behaviour of turbines under cavitating flow regimes supposed to be encountered on natural sites.

The LEGI has developed its own experimental facility which provides torque, longitudinal and transversal thrust measurements of a CFWT model (scale 1/5) for a water current in a rectangular duct. In the present paper, the overall capacity of this experimental facility is illustrated within the tests of the Darrieus, Gorlov [9] and Achard [10] water turbines. In a first part, the experimental setup is presented in detail. In a second part, the validity of the thrust measurements is demonstrated by a rigorous method based on permanent magnets. Finally, experimental results comparing the aforementioned turbines are shown.

2. Experimental apparatus

The hydrodynamic tunnel of the LEGI illustrated in Fig. 1, offers a test section of $0.250 \times 0.700 \text{ m}^2$ situated behind a squared convergent. The rectangular channel is inserted in a closed hydraulic loop of 30 m. In the test section, the flow velocity (U) varies from 1.0 m.s^{-1} to 2.8 m.s^{-1} . For the 0.175 m diameter tested turbines, it corresponds to a Reynolds number varying from 1.75×10^5 to 5.00×10^5 . This range corresponds approximately to a 0.5 m diameter turbine operating in a 1 m/s river current.

The measurement platform (Cf. Fig. 2) is mounted on the top of the test section. The line shaft is connected to the top of it (VII). The synchronous generator (III), which works as well as a motor, supplies the torque measurements. Indeed, for a rotational speed (N), the flow passing through the turbine increases (or decreases) the rotational speed of the line shaft. In order to regulate it, current intensity is dissipated (or injected) in the generator winding. The intensity is an image of the generator torque.

The measurement platform is installed on the test section top with four piezoelectric sensors (Cf. Fig. 2). As the line shaft, the platform (VII) and the test section are highly rigid, the piezoelectric sensors follow perfectly the instantaneous deformation of the turbine tested during its rotation.

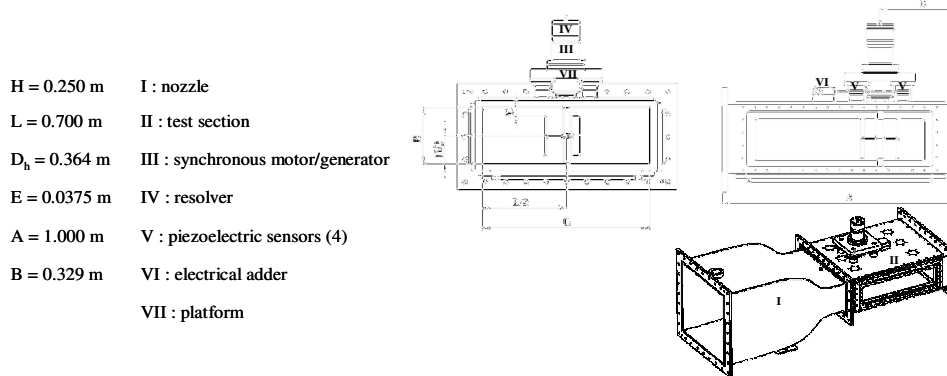


Fig. 1. Parts of the LEGI hydrodynamic channel.

Each piezoelectric sensor provides the three force components of the turbine. The global effort in a space direction at the point T (Cf. Fig. 2), is the combination of each effort measured with the sensors (noted F_{xi} , F_{yi} , F_{zi} in fig. 2). The three momentums of the force at T can be as well evaluated at the O point from the combination of each measured efforts for each independent sensor.

Nevertheless, for a symmetrical turbine (Darrieus or Achard water turbine) following the y plane, the component of the compression effort is zero; the measurement platform provides only two forces and one momentum (Cf. Fig.2).

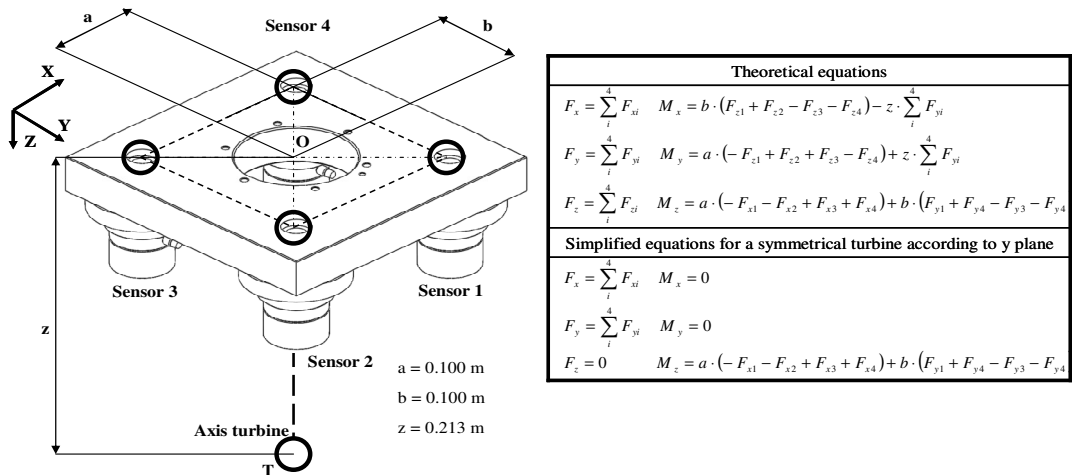


Fig. 2. The piezoelectric measurement platform

3. Analysis and validation of the measuring chain

The generator torque varies linearly with the delivered intensity; the proportional coefficient between the torque and the intensity, noted K , is insured by the manufacturer. The uncertainty about K has been evaluated to 1%.

The torque provided by the generator is the sum of three contributions: the water torque, the friction torque (due to bearing) and the inertial torque (due to the instantaneous variation of the angular speed). To obtain the water torque on the turbine, the friction and inertial torques are subtracted of the generator torque. The friction torques are evaluated before each test, without the turbine, in the same condition as if there was a turbine. The inertial torque is calculated according to the temporal variation of the angular speed and the inertia matrix of the rotating parts. To conclude, the torque uncertainty is about 3 to 5 %.

On the other hand, the uncertainty of the two efforts measured with the piezoelectric sensors depends strongly on the measurement environment. In order to estimate the uncertainty of the two thrusts and consequently of the moment around z axis, a magnetic approach is used (Cf. Fig. 3). Three permanent magnets spaced of 120° are fixed under the superior plate of the test section, it is the static part. One permanent magnet is fixed to the shaft, it is the mobile part. The gap between the static and the mobile part is between 0.001 and 0.002 m. While the shaft runs, two periodic repulsion transverse efforts and one periodic torque are applied to it.

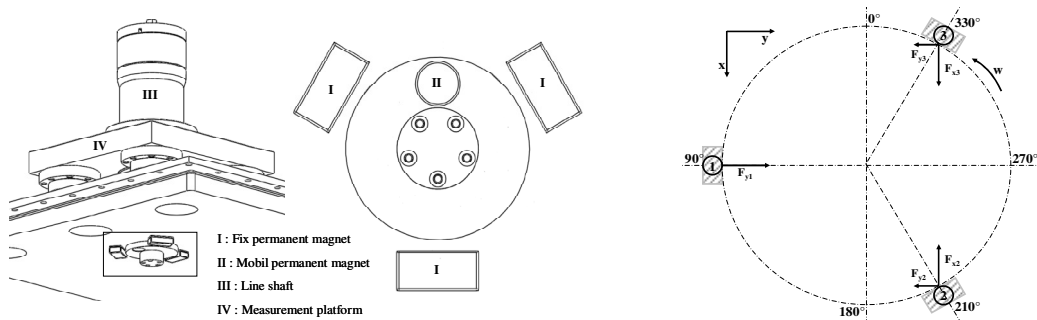


Fig. 3. Experimental facility with permanent magnets

The first step to evaluate the uncertainty of the measurement platform is to determine the repulsion strength between the two permanent magnets for several gaps. For that a hydraulic press is used. The results of this test are considered to be the reference for the uncertainty calculation. The second step is to measure, for several gaps, included between 0.001 and 0.002 m, the efforts in x and y directions between the 2 permanent magnets with the piezoelectric sensors. The gap between the two magnets is measured with rectangular gauge blocks. The measurement of the resultant effort is done when the mobile magnet is in front of the fixed magnet. The results of the two steps are listed in table 1.

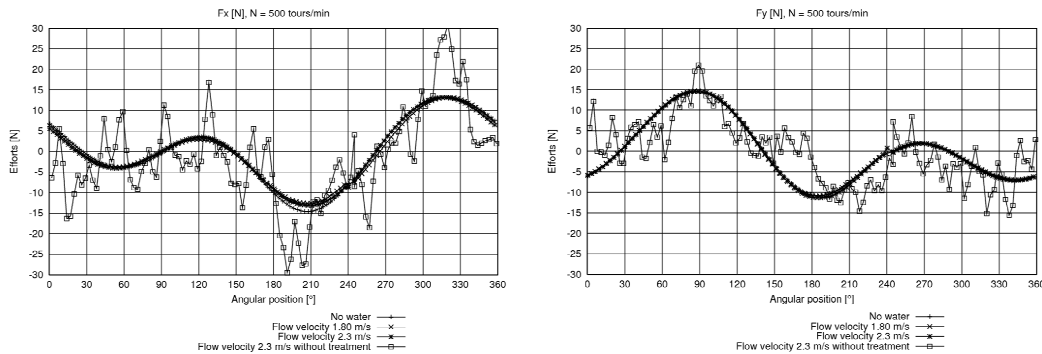
The efforts provided by the piezoelectric sensors are in concordance with the repulsion efforts measured with the hydraulic press (Cf. Table 1). The average uncertainty is about 3%.

Table 1

Analysis on the uncertainty of the measurement platform

Tests Series	Gap [m]	Measured forces – resultant effort [N]	References forces [N]	Error %
1	0.0016	21.5	20.7	3.9
2	0.0016	21.5	20.7	3.9
3	0.0017	20.5	20.0	2.5
4	0.0020	18.5	18.1	2.2
5	0.0020	18.3	18.1	1.1
6	0.0020	17.9	18.1	1.1

The following step is to determine the behaviour of the measuring chain in the same test conditions as for a water turbine: with a rotating shaft and a flow rate passing through the test section. For that, F_x and F_y forces are measured firstly without water; this results are the reference efforts. Secondly, the two efforts are measured with a flow rate in the test section.


 Figure 4 : Angular distribution of F_x (left) and F_y (right) efforts at 500 rpm.

The results of these two tests are illustrated in Fig. 4. The frequency sampling allows the measurement of one effort every three rotational degrees during 40 periods. The angular distributions of F_x and F_y correspond qualitatively and quantitatively to the expected force distribution shown in Fig. 3 right. At 90° , F_x value is equal to zero, whereas F_y reaches its maximum value. At 210° and 330° , F_x values are equal but opposite in direction, whereas F_y values are equal.

With a flow rate, the signals provided by the measuring chain are noised. A restriction of the spectral signal contents and a point by point average allow exempting the noise. With this treatment, F_x and F_y angular distributions are in perfect accordance with the waterless angular effort distributions.

However, torque calculation from measured forces is not suitable for two main reasons: firstly, permanent magnets do not provide a quantifiable torque for the dimensions of the measurement platform, and secondly, torque measurements with the generator are more efficient.

To conclude, the measuring chain provides, on the one hand, the measurement of two efforts with an uncertainty about 5%. In general, measuring chains are more efficient for high effort ranges. Consequently, the uncertainties evaluated for an effort range of -20 N to 20N (effort range of the permanent magnets) will be as good as those evaluated for a range of -100N to 100N, typically the order of magnitude of efforts on model turbines at 1/5 scale. On the other hand, the torque measurement uncertainty is about 5% too. The torque calculated from the measurement efforts is only an indicative torque.

4. Experimental results and analysis

Three turbines have been tested in the hydrodynamic channel. Fig. 5 illustrates the model turbines and Table 3 lists their reference values.

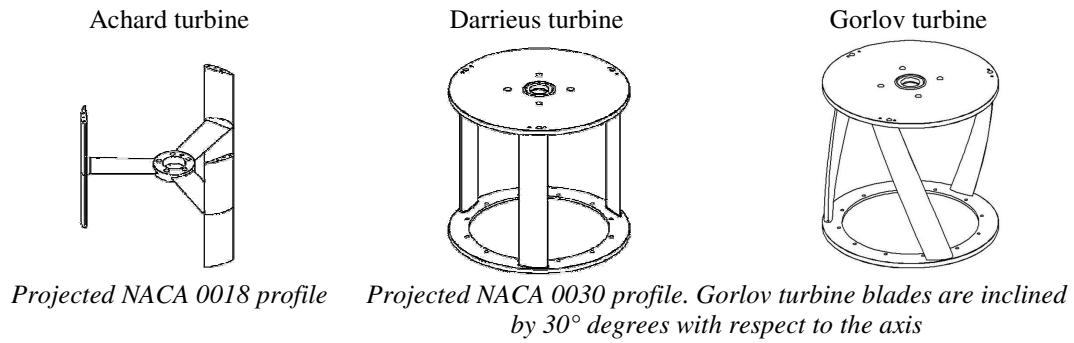


Fig. 5. Turbine description.

Table 3

Model reference values			
Height	$h = 0.175$	Radius	$r = 0.0875 \text{ m}$
Blade number	$n = 3$	Solidity	$\sigma = n \cdot c / r = 1.1$
Efficiency	$C_p = \frac{C_t \cdot N \cdot 2 \cdot \pi / 60}{0.5 \cdot \rho \cdot \pi \cdot 2 \cdot r \cdot h \cdot U^3}$	Specific speed	$\lambda = \frac{r \cdot \omega}{U}$

Fig. 6 left illustrates the evolution of the efficiency for the three turbines according to the tip speed ratio (λ) for a flow velocity equal to $2.3 \text{ m}\cdot\text{s}^{-1}$. All the three turbines have their optimum working point at λ equal to 2.00. The Achard turbine is the best with an efficiency of 33%. For each λ , especially for low and high values, the Achard turbine has the best efficiency. The Darrieus and Gorlov turbines have a restrained working range. The Gorlov turbine, which has helical blades, is the worst; its optimum efficiency is equal to 26%.

Fig. 6 right illustrates the angular torque distribution for the three turbines. The torque distribution is periodic with a frequency equal to three times the

rotational frequency. For the three turbines, the maximum torques are located at 90° , 210° and 330° and they are similar in value; however, the minimum torque values are different. The low torque value range of the Achard turbine is higher than the other turbines ones. This is the reason why the Achard turbine is better.

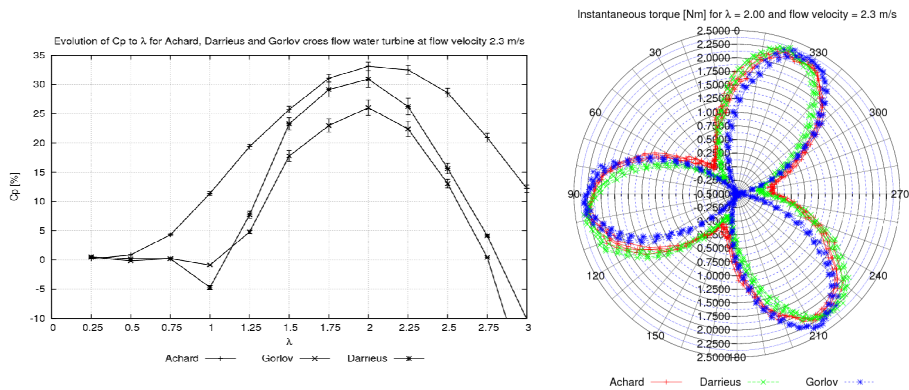


Fig. 6. Left, efficiency with λ ; right angular torque distribution for the three tested turbines.

Fig. 7 illustrates the angular distribution of the F_x and F_y efforts for the Achard, Darrieus and Gorlov water turbines. In general, the average longitudinal force is about 90N and the average transverse force is about 50 N. The F_y angular distribution is similar to the torque distribution (Fig. 6 left). For the turbine with straight blades (Achard and Darrieus turbines), the effort fluctuations are similar, however for a turbine with helical blades, the effort fluctuation is less marked. To conclude, in one revolution, the effort fluctuation range is about 100N for all tested turbines, which is non negligible for the mechanical fatigue.

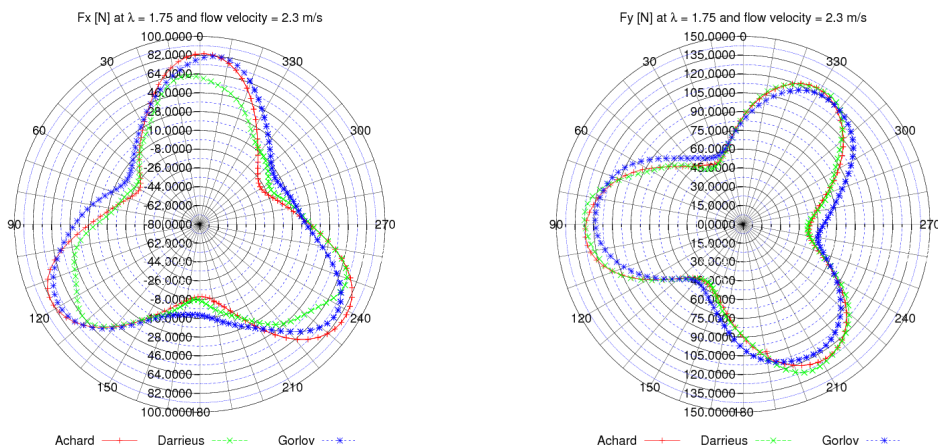


Fig. 7. Angular effort distribution at a flow velocity = 2.3 and $\lambda = 1.75$; left F_x , right F_y .

5. Conclusions

The LEGI disposes an efficient experimental facility for characterizing the hydrodynamic behaviour of CFWTs. Indeed, this experimental device provides the instantaneous torque measurement, as well as the longitudinal and transverse efforts, with an uncertainty of about 5%. The measuring chain allows a high data sampling, providing the measurement of one point every 3 rotational degrees of the CWFT. Among the tested turbines, in terms of performance, the Achard water turbine has the best efficiency and its operating range in λ is more spread than for the others. The helical blade of the Gorlov turbine allows reducing the effort fluctuations but this is reflected on a loss in efficiency. Even if just bare turbines have been presented in this paper, the hydrodynamic tunnel is also prepared to test other turbine configurations, including studies of the vertical and horizontal confinement, and the behaviour of turbines equipped with a channelling device. In addition, the hydrodynamic channel can also work under cavitating conditions.

REFERENCES

- [1]. *George Jean Marie Darrieus, Société anonyme pour l'exploitation des procédés Maurice Leblanc-Vickers*, "Turbine Having its Rotating Shaft Transverse to the Flow of the Current", Patent no° 1.835.018, Dec. 8, 1931.
- [2]. *Y. Takamatsu, A. Furukawa, K. Okuma and Y. Shimogama*, "Study on Hydrodynamic Performance, of Darrieus-type Cross-flow Water Turbine", Bulletin of JSME, **Vol. 28**, No. 240, June 1985.
- [3]. *Y. Takamatsu, A. Furukawa, K. Okuma, K. Takenouchi*, "Experimental Studies on a Preferable Blade Profile for High Efficiency and the Blade Characteristics of Darrieus-Type Cross-Flow Water Turbines", Bulletin of JSME, Serie II, **Vol. 34**, No. 2, 1991.
- [4]. *Y. Matsuda, M. Ikeda and K. Okuma, A. Furukawa and S. Watanabe*, "Experimental Study On Water Turbine Characteristics of Darrieus Type Runner with Staggered Blade Arrangement", The 7th Asian International Conference on Fluid Machinery, Fukuoka, Japan, 7-10-2003.
- [5]. *M. Shiono, K. Suzuki and S. Kiho*, "An Experimental Study of the Characteristics of a Darrieus Turbine for Tidal Power Generation", Electrical Engineering in Japan, **Vol. 132**, No. 3, 2000.
- [6]. *B. Kirke, L. Lazauskas*, "Variable Pitch Darrieus Water Turbines", Journal of Fluid Science and Technology, **Vol. 3**, No. 3, 2008.
- [7]. *T. Faure, B. Pratte and D. Swan*, "The Darrieus Hydraulic Turbine – Model and Field Experiments", Proc. 4th ASME International Symposium for Hydro Power and Fluid Machinery, San Francisco, 1986
- [8]. *I. Paraschivoiu*, "Wind Turbine Design With Emphasis on Darrieus Concept", Polytechnic International Press.
- [9]. *A. Gorlov*, "Helical Turbines for the Gulf Stream: Conceptual Approach to Design of a Large-Scale Floating Power Farm", Marine Technology, **Vol. 35**, No. 3, 1998.
- [10]. *J. L. Achard, T. Maître*, « Hydraulic Turbomachine », Patent no : FR04 50209, Applicant INPG (FR), Fev. 4, 2004